JACS
JOURNAL OF THE AMERICAN CHEMICAL SOCIETY

Communication

pubs.acs.org/JACS

Proton-Coupled Electron Transfer in Azobenzene/Hydrazobenzene Couples with Pendant Acid–Base Functions. Hydrogen-Bonding and Structural Effects

Jean-Michel Savéant* and Cédric Tard*

Laboratoire d'Electrochimie Moléculaire, UMR 7591, CNRS, Université Paris Diderot, Sorbonne Paris Cité, 15 rue Jean-Antoine de Baïf, F-75205 Paris Cedex 13, France

Supporting Information

ABSTRACT: Electron transfer in azobenzene derivatives bearing two carboxylic acid groups is coupled with intramolecular proton transfer in a stepwise manner in the title $2e^- + 2H^+$ redox couple. The presence of the pendant acid–base functions pushes the redox chemistry of the azo/hydrazo couple toward positive potentials by as much as 0.75 V. This is essentially the result of H-bonding of one of the nitrogen atoms by the neighboring carboxylic group and H-bonding of one carboxylate by the neighboring protonated nitrogen atom. The two electron-transfer reactions, particularly the second one, are accompanied by strong structural changes, which results in the occurrence of a square scheme mechanism in which electron transfer and structural change are not concerted. These are typical phenomena that are likely to be encountered when attempting to boost proton-coupled electron-transfer stoichiometric or catalytic processes by installing pendant acid–base functionalities in the close vicinity of the reacting center.

There are several reasons for the long-standing interest aroused by azo/hydrazo couples:

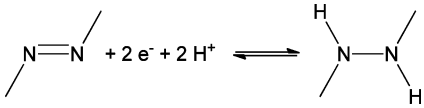

One has to do with the general scheme of N–N multiple-bond activation. A seminal example is the electrochemical reduction of the nitrogen molecule (N_2) into ammonia (NH_3), which is one of the most arduous challenges in contemporary chemistry.[1] This $6e^- + 6H^+$ reaction has attracted much attention over the past decades, particularly due to the fact that biological N_2 fixation can be performed at ambient pressure and temperature by nitrogenase enzymes, with a heterometallic iron/molybdenum/sulfur/carbon active cluster.[2] Mechanistic studies of the strong N–N triple-bond activation are thus imperative to unravel general trends toward the design of new types of electrocatalysts.[3]

Another motive deals with the microbial degradation of azo dyes. In biology, azoreductases are enzymes that catalyze the $4e^- + 4H^+$ anaerobic reduction of azobenzene derivatives by converting azo bonds to aniline moieties. This enzymatic reaction is important, considering its role in detoxification of azo dyes produced by the textile industry[4] and activation of anti-inflammatory azo pro-drugs.[5] In these systems, the bond cleavage requires two reductive cycles, with the reduction of FMN to $FMNH_2$ by NADPH to give the hydrazo intermediate in the first step and release of aniline in a second reductive step.[6] Researchers are thus focusing on the design of novel dyes/pro-drugs in which the biodegradability (i.e., the cleavage of the azo bond by azoreductases) is adjusted by the chemical structure of the molecule.[4c]

The electrochemistry of azo/hydrazo couples, specifically the azobenzene/hydrazobenzene couple, has been investigated for a long time,[7−13] mostly by means of cyclic voltammetry (CV) in aprotic media (acetonitrile and *N,N′*-dimethylformamide (DMF)), with the aim of assessing the number of electron-transfer reactions, their degree of reversibility, and the role of added Brönsted acids. The latter aspect is at the origin of our interest in the electron-transfer chemistry of azobenzene/hydrazobenzene couples in the framework of proton-coupled electron transfer (PCET) reactions.[14] More specifically, the present work concerns the role of proximal acid–base groups attached to the same structure as the PCET substrate: do they act as H-bond promoters and/or proton donors? This question is currently attracting active attention in the framework of stoichiometric[15−18] and catalytic reactions connected with the resolution of modern energy challenges.[19,20]

Chart 1. Structures of the Azobenzene (A1) and Hydrazobenzene (C3) Molecules Bearing Attached Carboxylic and Carboxylate Groups, Respectively, and of the Methyl Ester of A1 (A-Me)

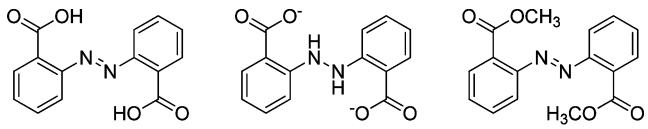

A1 C3 A-Me

The structures of the azobenzene and hydrazobenzene that we investigated are shown in Chart 1. They correspond to the compounds noted **A1** and **C3** in the mechanistic Scheme 1.

The cyclic voltammetric responses (see the Supporting Information (SI) for experimental details) observed at low scan rate (Figure 1) confirm that the azo and hydrazo compounds

Received: May 8, 2014
Published: June 12, 2014

 © 2014 American Chemical Society dx.doi.org/10.1021/ja504484a | *J. Am. Chem. Soc.* 2014, 136, 8907–8910

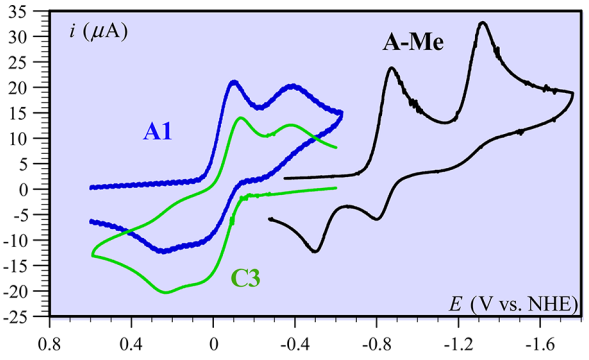

Figure 1. Cyclic voltammetry of 1 mM **A1**, **C3**, and **A-Me** (see Chart 1) in DMF + 0.1 M n-NBu_4BF_4 at 0.2 V/s.

are redox partners: the reverse CV trace of the azo compound is similar to the forward trace of the hydrazo compound, and *vice versa*. Each of the two compounds exhibits two waves, with the first close to being reversible, as do the simple azo- and hydrazobenzenes in similar conditions.[7,9−11] This is also the case for the methyl ester of the azo compound (Figure 1). The reduction potentials of **A1** and oxidation potentials of **C3** are, however, considerably shifted toward positive values, by ca. 800 mV, as compared to those of **A-Me** or the simple azo- and hydrazobenzenes. Since inductive effects are expected to be of the same order of magnitude in **A1** and **A-Me**, it appears that the presence of the two carboxylic groups in **A1** and carboxylate groups in **C3** is responsible for this huge change in the redox chemistry of the azo/hydrazo couple, which is therefore likely to be due to intramolecular proton transfer and/or intramolecular H-bonding.

Among the nine possible intermediates (see SI) of the two-proton and two-electron transfers, density functional theory (DFT) calculations (see SI) revealed that only the intermediates shown in Scheme 1 are not too unreasonably high in energy to partake in the reaction, leading to a classical "ECEC mechanism",[21] or even a classical "ECE mechanism",

Scheme 1. Mechanistic Reaction Scheme Including the Electron- and Proton-Transfer Steps Together with Views of Each Molecule Showing Their Degree of Torsion around the N−N Bond

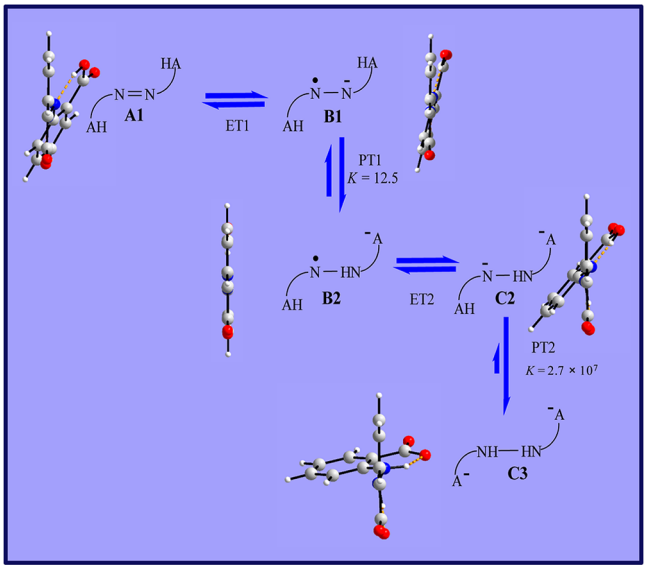

since the last step is likely to be slow enough to be neglected within the time scale of CV, as discussed below. We may thus assign (see Figures 1 and 2) the first group of waves to the reduction of **A1** to **B2** (and reverse oxidation) and the second group of waves to the reduction of **B2** to **C3** (and reverse oxidation). The DFT calculations also indicate that the anion radical **B2**, which derives from **B1** by the transfer of the proton of one carboxylic group to the neighboring nitrogen atom, is only slightly more stable than its parent (equilibrium constant 12.5). This proton transfer is likely to be rapid in both directions because the structure does not change much from **B1** to **B2**. It follows that the protonation reaction counts for ca. 60 mV in the shift of the reduction potential over a total value of 800 mV. The total stabilization of the anion radicals by H-bonding thus reaches the very large value of 740 mV. It involves H-bonding of one of the nitrogen atoms by the neighboring carboxylic group in **B1** and H-bonding of one carboxylate by the neighboring protonated nitrogen atom in **B2**. It is interesting to note that the large increase in the strength of H-bonding from the starting azo compound, **A1**, to the anion radical, **B1**, is the result of the change in the molecular structure accompanying electron transfer that makes the distance between each nitrogen atom and the hydrogen atom of the proximal carboxylic acid change from 1.75 to 1.60 Å, while the O−H distance in the carboxylic groups remains almost constant (Chart 2).

Chart 2. Variation of the H-Bonding Distances (in Å) upon Electron Transfer from A1 to B1[a]

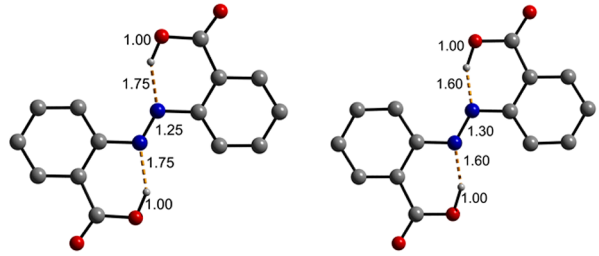

[a]Color-coding of the atoms: gray, carbon; red, oxygen; blue, nitrogen.

Another important remark derives from the quasi-absence of H/D isotope effects. The CV responses are indeed almost the same in the presence of 1% CH_3OH and 1% CD_3OD (see SI). The small changes may be attributed to marginal thermodynamic effects. It may thus be concluded from this absence of kinetic H/D isotope effect that the coupling between proton and electron transfer follows stepwise pathways rather than concerted pathways,[14] as sketched in Scheme 1 (concerted pathways would imply going directly from **A1** to **B2** and from **B2** to **C3**).

The DFT calculations also showed (see insets in Scheme 1) that the radical anions (compounds **B1** and **B2** in Scheme1) are almost planar, whereas the starting azo compound exhibits torsion around the N=N bond. This is much more pronounced in the dianions (compounds **C2** and **C3** in Scheme 1). It follows that we must envisage that electron transfer ET2 may not be a single-step process in which the accompanying strong structural change would not be concerted with electron transfer, but would involve discrete intermediates,[22] as shown in Scheme 2 (**B′2**).

dx.doi.org/10.1021/ja504484a | J. Am. Chem. Soc. 2014, 136, 8907−8910

Scheme 2. Stepwise and Concerted Mechanisms in the Reactions Where Electron Transfer Is Accompanied by a Strong Structural Change[a]

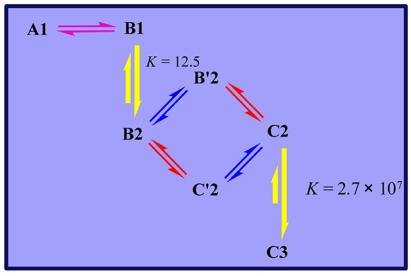

[a]Color-coding of the arrows: blue, electron transfers with little structural changes; red, structural changes; magenta, electron transfer concerted with a modest structural change; yellow, proton transfer. The values of the equilibrium constants shown in the diagram were obtained from DFT calculation (see SI).

The **C2** → **C3** reaction, albeit thermodynamically favorable, may be neglected within the CV time scale since it is likely to be very slow, in view of the considerable change of structure it involves.

We may finally attempt to simulate the CV responses obtained at various scan rates that are reported in the left-hand column of Figure 2. The main trends of the CV responses as a function of the scan rates are reproduced by simulation of Scheme 1, completed by Scheme 2, to obtain the values of the thermodynamic and kinetic constants listed in Table 1.[23]

Table 1. Constants for Simulation According to Schemes 1 and 2

Reaction	Thermodynamic and kinetic constants [a]
ET1 **A1** ⇌ **B1**	$E^0 = 0.002$, $\alpha = 0.5$, $k_S = 0.006$
PT1 **B1** ⇌ **B2**	$K = 13$, $k_f = 10^{10}$, $k_b = 8\times10^8$
ET2	
B2 ⇌ **B'2**	$E^0 = -0.42$, $\alpha = 0.5$, $k_S = 0.001$
B'2 ⇌ **C2**	$K = 10^3$, $k_f = 10^6$, $k_b = 10^3$
C'2 ⇌ **C2**	$E^0 = -0.13$, $\alpha = 0.5$, $k_S = 0.002$
B2 ⇌ **C'2**	$K = 3\times10^{-2}$, $k_f = 10^3$, $k_b = 3.6\times10^6$

[a]Standard potentials in V vs NHE, standard rate constant in cm s^{-1}, and first-order homogeneous rate constants in s^{-1}.

In summary, four main conclusions emerge from the present study. (i) The mutual $2e^- + 2H^+$ reaction of the azo/hydrazo couple involves the intramolecular displacement of the protons borne by the pendant carboxylic/carboxylate functionalities placed in the vicinity of the azo/hydrazo group. These intramolecular electron and proton transfers occur in a stepwise manner, rather than concertedly. (ii) The presence of the pendant carboxylic/carboxylate functionalities in the vicinity of the azo/hydrazo N−N group produces a considerable positive shift in the characteristic standard potentials, as large as ca. 0.75 V. Rather than being caused by intramolecular proton transfer, this is essentially the result of H-bonding of one of the nitrogen atoms by the neighboring carboxylic group and H-bonding of one carboxylate by the neighboring protonated nitrogen atom. (iii) Intramolecular proton-coupled electron transfer in these

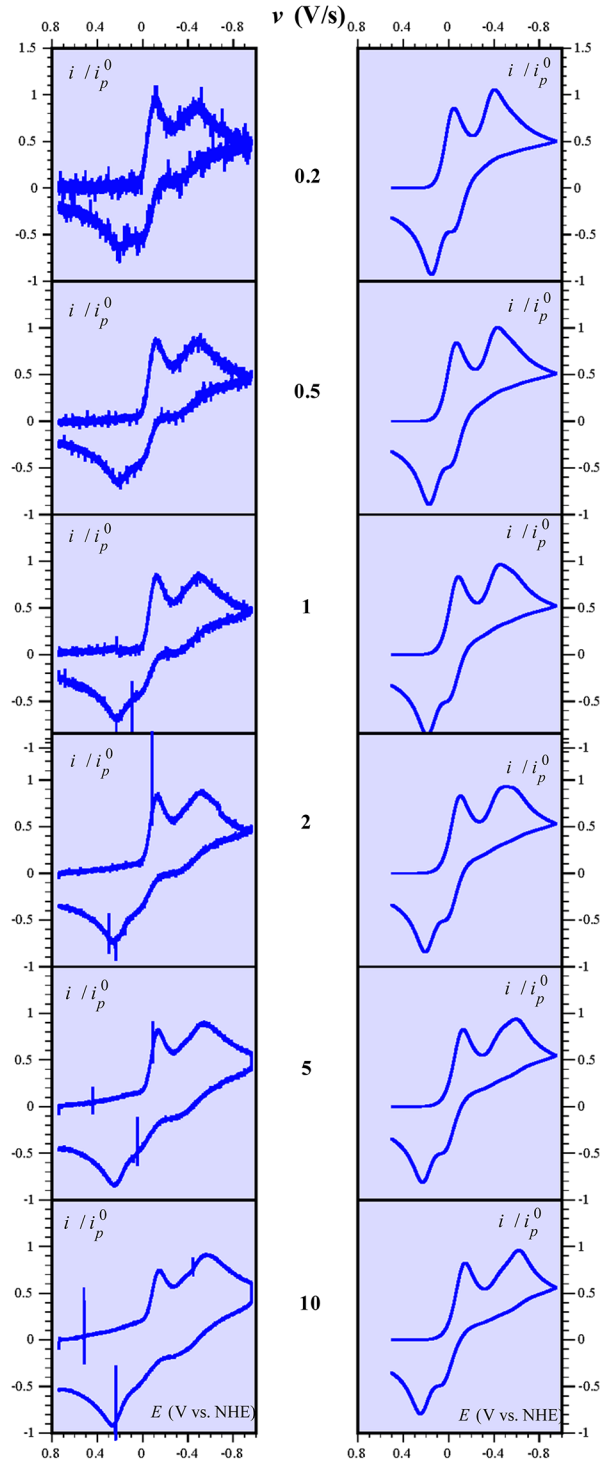

Figure 2. Cyclic voltammetry of 1 mM **A1** in DMF + 0.1 M *n*-NBu_4BF_4 as a function of the scan rate. Left, experimental; right, simulated (see text and Table 1). The current is normalized toward the peak current of a one-electron reversible Nernstian wave, $i_p^0 = 0.446FSC^0D^{1/2}(Fv/RT)^{1/2}$, where v is the scan rate in V/s, S is the electrode surface area (0.07 cm^2), and C^0 is the azobenzene concentration (1 mM).

molecules is accompanied by considerable structural changes. Injection of one electron into the initially distorted azo compound flattens out the molecule. The resulting anion radical keeps the same geometry after intramolecular migration of one proton to one of the nitrogens of the azo group. The

dx.doi.org/10.1021/ja504484a | J. Am. Chem. Soc. 2014, 136, 8907−8910

most dramatic distortion, however, occurs upon injection of a second electron and intramolecular displacement of one proton. Migration of the second proton produces an even more distorted dianion. (iv) These strong structural changes have important mechanistic and kinetic consequences. While during the first electron uptake the change in structure seems to occur in concert with electron transfer, this is not the case during the second electron transfer, which involves a much larger distortion of the molecular frame. In this case, the reaction occurs according to a square-scheme mechanism, which involves as intermediates a dianion that has the same flat structure as the initial anion radical and an anion radical that has the same distorted structure as the final dianion.

We hope that these findings will help in understanding the numerous existing attempts to boost PCET stoichiometric or catalytic processes by installing pendant acid–base functionalities in the close vicinity of the reacting center and in devising new such systems.

■ ASSOCIATED CONTENT

Supporting Information

Experimental details, DFT calculations, and procedures. This material is available free of charge via the Internet at http://pubs.acs.org.

■ AUTHOR INFORMATION

Corresponding Authors

saveant@univ-paris-diderot.fr
cedric.tard@univ-paris-diderot.fr

Notes

The authors declare no competing financial interest.

■ ACKNOWLEDGMENTS

Aurélie Perrier-Pineau and Arnaud Fihey are thanked for helpful advice and suggestions on the DFT calculations.

■ REFERENCES

(1) *Nitrogen fixation at the millennium*; Leigh, G. J., Ed.; Elsevier: Amsterdam, 2002.

(2) Hoffman, B. M.; Lukoyanov, D.; Yang, Z.-Y.; Dean, D. R.; Seefeldt, L. C. *Chem. Rev.* **2014**, *114*, 4041.

(3) Hoffman, B. M.; Lukoyanov, D.; Dean, D. R.; Seefeldt, L. C. *Acc. Chem. Res.* **2013**, *46*, 587.

(4) (a) Stolz, A. *Appl. Microbiol. Biotechnol.* **2001**, *56*, 69. (b) Saratale, R. G.; Saratale, G. D.; Chang, J. S.; Govindwar, S. P. *J. Taiwan Inst. Chem. E* **2011**, *42*, 138. (c) Solís, M.; Solís, A.; Pérez, H. I.; Manjarrez, N.; Flores, M. *Process Biochem.* **2012**, *47*, 1723.

(5) Wiggins, J. B.; Rajapakse, R. *Exp. Opin. Drug Met.* **2009**, *5*, 1279.

(6) Ryan, A.; Laurieri, N.; Westwood, I.; Wang, C.-J.; Lowe, E.; Sim, E. *J. Mol. Biol.* **2010**, *400*, 24.

(7) Sadler, J. L.; Bard, A. J. *J. Am. Chem. Soc.* **1968**, *90*, 1979.

(8) Neta, P.; Levanon, H. *J. Phys. Chem.* **1977**, *81*, 2288.

(9) Bellamy, A. J.; MacKirdy, I. S.; Niven, C. E. *J. Chem. Soc., Perkin Trans. 2* **1983**, 183.

(10) Cheng, S.; Hawley, M. D. *J. Org. Chem.* **1985**, *50*, 3388.

(11) (a) Ingemann, S.; Nielsen, M. F.; Hammerich, O. *Acta Chem. Scand.* **1988**, *42b*, 583. (b) Ingemann, S.; Larsen, K. V.; Haugshøj, K. B.; Hammerich, O. *Acta Chem. Scand.* **1989**, *43*, 981.

(12) Sanchez, P. D. A.; Evans, D. H. *J. Electroanal. Chem.* **2010**, *638*, 84.

(13) Benniston, A. C.; Harriman, A.; Yang, S.; Harrington, R. W. *Tetrahedron Lett.* **2011**, *52*, 5315.

(14) (a) Costentin, C. *Chem. Rev.* **2008**, *108*, 2145. (b) Costentin, C.; Robert, M.; Savéant, J.-M. *Chem. Rev.* **2010**, *110*, PR1. (c) Savéant, J.-M. *Annu. Rev. Anal. Chem.* **2014**, DOI: http://www.annualreviews.org/doi/abs/10.1146/annurev-anchem-071213-020315.

(15) (a) Gómez, M.; González, F. J.; González, I. *J. Electroanal. Chem.* **2005**, *578*, 193. (b) Alligrant, T. M.; Alvarez, J. C. *J. Phys. Chem. C* **2011**, *115*, 10797. (c) Astudillo, P. D.; Valencia, D. P.; González-Fuentes, M. A.; Díaz-Sánchez, B. R.; Frontana, C.; González, F. J. *Electrochim. Acta* **2012**, *81*, 197.

(16) (a) Ge, Y.; Lilienthal, R. R.; Smith, D. K. *J. Am. Chem. Soc.* **1996**, *118*, 3976. (b) Ge, Y.; Miller, L.; Ouimet, T.; Smith, D. K. *J. Org. Chem.* **2000**, *65*, 8831. (c) Clare, L. A.; Rojas-Sligh, L. E.; Maciejewski, S. M.; Kangas, K.; Woods, J. E.; Deiner, L. J.; Cooksy, A.; Smith, D. K. *J. Phys. Chem. C* **2010**, *114*, 8938. (d) Clare, L. A.; Pham, A. T.; Magdaleno, F.; Acosta, J.; Woods, J. E.; Cooksy, A. L.; Smith, D. K. *J. Am. Chem. Soc.* **2013**, *135*, 18930.

(17) (a) Rhile, I. J.; Mayer, J. M. *J. Am. Chem. Soc.* **2004**, *126*, 12718. (b) Rhile, I. J.; Markle, T. F.; Nagao, H.; DiPasquale, A. G.; Lam, O. P.; Lockwood, M. A.; Rotter, K.; Mayer, J. M. *J. Am. Chem. Soc.* **2006**, *128*, 6075. (c) Markle, T. F.; Mayer, J. M. *Angew. Chem. Int. Ed.* **2008**, *47*, 564. (d) Warren, J. J.; Tronic, T. A.; Mayer, J. M. *Chem. Rev.* **2010**, *110*, 6961. (e) Markle, T. F.; Rhile, I. J.; Mayer, J. M. *J. Am. Chem. Soc.* **2011**, *133*, 17341. (f) Markle, T. F.; Tronic, T. A.; DiPasquale, A. G.; Kaminsky, W.; Mayer, J. M. *J. Phys. Chem. A* **2012**, *116*, 12249. (g) Schrauben, J. N.; Cattaneo, M.; Day, T. C.; Tenderholt, A. L.; Mayer, J. M. *J. Am. Chem. Soc.* **2012**, *134*, 16635.

(18) (a) Costentin, C.; Robert, M.; Savéant, J.-M. *J. Am. Chem. Soc.* **2006**, *128*, 4552. (b) Costentin, C.; Robert, M.; Savéant, J.-M. *J. Am. Chem. Soc.* **2006**, *128*, 8726. (c) Costentin, C.; Robert, M.; Savéant, J.-M. *J. Am. Chem. Soc.* **2007**, *129*, 9953. (d) Costentin, C.; Hajj, V.; Robert, M.; Savéant, J.-M.; Tard, C. *Proc. Natl. Acad. Sci. U.S.A.* **2011**, *108*, 8559. (e) Costentin, C.; Robert, M.; Savéant, J.-M.; Tard, C. *Phys. Chem. Chem. Phys.* **2011**, *13*, 5353. (f) Bonin, J.; Costentin, C.; Robert, M.; Savéant, J.-M.; Tard, C. *Acc. Chem. Res.* **2012**, *45*, 372; **2013**, *46*, 1910.

(19) (a) Wilson, A. D.; Newell, R. H.; McNevin, M. J.; Muckerman, J. T.; DuBois, M. R.; DuBois, D. L. *J. Am. Chem. Soc.* **2006**, *128*, 358. (b) Wilson, A. D.; Shoemaker, R. K.; Miedaner, A.; Muckerman, J. T.; DuBois, D. L.; DuBois, M. R. *Proc. Natl. Acad. Sci. U.S.A.* **2007**, *104*, 6951. (c) O'Hagan, M.; Shaw, W. J.; Raugei, S.; Chen, S.; Yang, J. Y.; Kilgore, U. J.; DuBois, D. L.; Bullock, R. M. *J. Am. Chem. Soc.* **2011**, *133*, 14301. (d) Raugei, S.; Chen, S. T.; Ho, M. H.; Ginovska-Pangovska, B.; Rousseau, R. J.; Dupuis, M.; DuBois, D. L.; Bullock, R. M. *Chem.—Eur. J.* **2012**, *18*, 6493. (e) Liu, T. B.; DuBois, D. L.; Bullock, R. M. *Nat. Chem.* **2013**, *5*, 228.

(20) Costentin, C.; Drouet, S.; Robert, M.; Savéant, J.-M. *Science* **2012**, *338*, 90.

(21) Savéant, J.-M. *Elements of molecular and biomolecular electrochemistry: an electrochemical approach to electron transfer chemistry*; John Wiley & Sons: Hoboken, NJ, 2006; Chap. 2.

(22) Carefully characterized examples of the occurrence of such stepwise mechanisms of electron transfers accompanied by strong structural changes have been reported: (a) Hong, S. H.; Evans, D. H.; Nelsen, S. F.; Ismagilov, R. F. *J. Electroanal. Chem.* **2000**, *486*, 75. (b) Macías-Ruvalcaba, N. A.; Evans, D. H. *J. Phys. Chem. B* **2006**, *110*, 24786. (c) Macías-Ruvalcaba, N. A.; Evans, D. H. *Chem.—Eur. J.* **2007**, *13*, 4386. (d) Evans, D. H. *Chem. Rev.* **2008**, *108*, 2113.

(23) The simulations do not reproduce exactly the experiments in terms of vertical location of the second waves. This often happens, probably because the diffusion regime at a glassy carbon electrode is not exactly a linear diffusion regime as assumed in the simulations. It is reassuring that the shape (splitting–overlapping) and location of the second wave system are well reproduced by the simulations.